Chamber inhibitors of steel corrosion based on lauric acid, octadecylamine, and their mixtures

A.Yu. Luchkin, I.V. Tsvetkova, I.A. Kuznetsov, O.S. Makarova, O.A. Goncharova, N.N. Andreev* and S.S. Vesely

A.N. Frumkin Institute of Physical Chemistry and Electrochemistry, Russian Academy of Sciences, Leninsky pr. 31, 119071 Moscow, Russian Federation
**E-mail: n.andreev@mail.ru*

Abstract

The protective effect of chamber corrosion inhibitors of steel based on lauric acid has been studied by electrochemical and corrosion methods. It has been found that its protective action can be enhanced by addition of octadecylamine or combinations of octadecylamine with benzotriazole or derivatives of the latter such as tolyltriazole and chlorobenzotriazole. All the formulations studied and their components have a blocking-activating mechanism of action, with predominance of the activation mechanism. The protective effect of the mixed inhibitors studied significantly exceeds that of their components. However, analysis of the mutual effects of the components indicates the lack of their synergistic interactions. Ellipsometric methods show that adsorption of the inhibitors studied hinders or prevents the growth of oxide on steel during the chamber treatment (CT). Nanoscale adsorption films are formed on the steel surface during the CT of steel with the inhibitors studied. There is no unambiguous relationship between their thickness and the protective aftereffect of chamber inhibitors, but the most efficient inhibitors form adsorption layers with a thickness of 10 nanometers or more.

Received: October 31, 2022. Published: December 6, 2022 doi: 10.17675/2305-6894-2022-11-4-21

Keywords: *atmospheric corrosion, chamber inhibitors, lauric acid, vapor-phase protection of steel.*

Introduction

Chamber corrosion inhibitors (CIN) are a new promising class of vapor-phase inhibitors intended for temporary protection of metals [1–5]. The use of CIN implies the treatment of products in inhibitor vapors at an elevated temperature where compounds that have low vapor pressure under normal conditions acquire high volatility. This process is called chamber treatment (CT). During this treatment, inhibitor vapors are adsorbed on the metal and form thin adsorption layers with a high protective aftereffect.

The chamber protection of metals has a number of significant advantages over the traditional vapor-phase protection of metals by volatile inhibitors (VCI). First, CIN do not require sealing the volume with the inhibitor and metal items for the entire storage period. CT is performed in sealed chambers, but its duration usually does not exceed one hour. After

that, the metal products are removed from the chambers. Second, chamber treatment is more cost-effective. In fact, the inhibitor is consumed only for the formation of nanoscale films on the surface of metal items. Third, CT is a very safe process in which the CINs are located only in the working chamber and do not directly contact either with the personnel engaged in corrosion protection operations or with the environment.

It has been shown in our works [6–11] that the chamber method can provide efficient protection of various metals and alloys from atmospheric corrosion. At the same time, in most cases, mixed CINs have better corrosion protection properties than their individual components.

Previously [12] we considered the possibility of steel protection and properties of CIN based on mixtures of lauric acid (LA), urotropine (UR) and benzotriazoles, namely 1,2,3-1*H*-benzotriazole (BTA), tolyltriazole (TTA) and 5-chloro-1,2,3-1*H*-benzotriazole (CBTA). The purpose of this work was to estimate the protective properties of similar mixtures where UR was replaced by octadecylamine (ODA). Note that ODA is a promising CIN [2, 3, 7, 9].

1. Experimental

1.1. Samples and electrodes

Samples and electrodes made of St3 steel were used in the studies. The steel composition matches the corresponding standard [13].

The flat specimens intended for corrosion tests had dimensions of 30×50×3 mm. Each specimen had a hole for mounting in test cells and chambers. Cylindrical electrodes were 10 mm in diameter. One of their cross-cuts had a hole with a thread for a mounting rod. Electrodes were embedded in Teflon casings in order to protect their side surfaces from interaction with the electrolyte during the tests. The bottom cross-cut of a cylinder served as the working surface.

Before the experiments, the working surfaces of the samples and electrodes were cleaned with sandpaper of various grain sizes, degreased with acetone, thoroughly washed with water, and dried.

Samples and electrodes prepared as described above were mounted in sealed glass vessels with a capacity of 0.6 liters containing a weighed amount of a CIN (0.5 g) or without it. The vessels were placed in a SNOL 50/350 drying oven heated to 120°C. The metal treatment time was 1 h. In accordance with [3, 9, 12], this temperature and CT duration are sufficient for the formation of protective adsorption films on steel. After exposure in the drying oven, the vessels were removed and cooled to room temperature. The samples and electrodes were removed from the atmosphere containing the CIN vapors and kept for 24 hours under ambient conditions.

1.2. Electrochemical studies

1.2.1. Voltammetric tests

Voltammetric experiments were performed using an IPC-pro potentiostat (Russian Federation) and a standard three-electrode cell with divided electrode spaces. A platinum wire served as the auxiliary electrode. The potentials (E) were measured against a saturated silver/silver chloride reference electrode and converted to the normal hydrogen scale. Experiments were carried out in borate buffer solution (pH 7.36) containing 0.001 M sodium chloride. Electrodes were placed in a cell with the electrolyte, kept for 5 min, and polarized anodically from the established potential (E_0) at a sweep rate of 0.2 mV/s. The protective properties of the CIN were characterized by pitting potentials (E_{pt}), breakdown potentials (E_{br}), and anti-pitting basis ($\Delta E = E_{pt} - E_0$). E_{pt} was determined as the potential at which current oscillations appeared on the polarization curves or as E_{br} if no oscillations were observed. E_{br} was determined as the potential where the anodic current density (i) reached 5 μA/cm^2.

1.2.2. Electrochemical impedance spectroscopy

Electrochemical impedance spectra were recorded using a potentiostat of the same brand as indicated above and a frequency response analyzer (FRA) manufactured in the Russian Federation. The experiments were carried out using a cell, electrodes, and conditions similar to those used in the polarization experiments. The frequency was varied from 0.1 to 10^5 Hz. Electrochemical impedance parameters were calculated using the equivalent circuit that is widely used for various metals and alloys [2–10]:

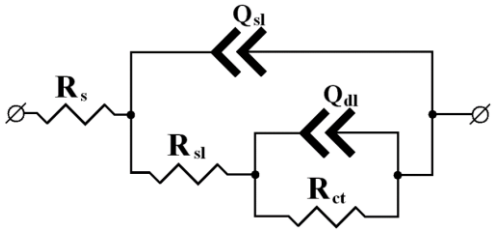

where R_s is the resistance of the bulk electrolyte between the auxiliary and working electrodes that does not affect the electrode processes and depends on the conductivity of the medium and the cell geometry; R_{sl} is the resistance of the surface layers (oxide–hydroxide and adsorption ones); R_{ct} is the polarization resistance characterizing the electrochemical kinetics of the corrosion process; Q_{sl} is the constant phase element characterizing the capacitance of surface oxide–hydroxide layers and/or adsorption layers; and Q_{dl} is the constant phase element that reflects the capacitance of the double electric layer. The impedance of the constant phase element is described by the equation:

$$Z_Q = A^{-1}(j\omega)^{-n},$$

where A is the proportionality factor; j is the imaginary unit; ω is the complex frequency associated with the alternating current frequency; and n is the exponential factor, $0 \le |n| \le 1$.

The results were processed to determine the equivalent circuit parameters using Dummy Circuits Solver software, version 2.1. The fit between experimental and calculated data was no worse than 98%.

The degree of steel electrode protection was calculated by the formula:

$$Z = \frac{(R_{inh} - R_{bg})}{R_{inh}} \cdot 100\%,$$

where R_{bg} and R_{inh} is the total resistance of the "steel–electrolyte" interphase interaction that includes R_{ct} and R_{sl} after thermal treatment (TT) of the electrode in the absence and in the presence of a CIN, respectively.

1.3. Corrosion tests

The protective aftereffect (PAE) of the surface layers formed during CT was estimated at 100% relative humidity with recurrent moisture condensation. The samples were mounted by polymer hooks to the lids of sealed glass cells so as to prevent their contact with each other and with the cell walls. The volume of each cell was 0.6 L. Hot water (0.15 L, 50°C) was poured into each cell, which caused abundant moisture condensation on the samples. After that, the cells were placed into a SNOL 50/350 thermostatic cabinet where the following temperatures were maintained every day: 40°C for 8 h and 20°C for 16 h. The samples were visually examined every hour without opening the cells, for two days from the beginning of the tests and every 6 hours in the subsequent days. The time (τ) until indications of corrosion appeared on the metal was recorded.

1.4. Ellipsometry

The thicknesses (*d*) of films formed on the metal during the CT were determined using a Gartner manual ellipsometer with light beam modulation and an advanced light detector. An LSM-S-111-10-NNP25 solid-state laser with diode pumping and a wavelength of 540 nm served as the radiation source. The changes in ellipsometric angles Δ and ψ were measured during the experiment. These values were compared to the values calculated using the Ellipsometry Calculation Spreadsheet program [14] for various refraction indices and surface layer thicknesses. The layer thicknesses were varied to find the best fit between the calculated and experimental Δ and ψ values. The three-layer approximation model (metal–oxide layer–adsorption film) was used to process the data.

2. Results and Discussion

2.1. Electrochemical studies

2.1.1. Polarization curves

The shape of anodic polarization curves of steel samples in the initial state (IS) and after treatment are typical of the passive metal (Figure 1).

The E_0 value of a sample in the IS, *i.e.*, one that did not undergo thermal treatment (TT) or CT, was about 0.1 V. Almost immediately after the beginning of the potential sweep in the anodic direction, current oscillations appeared on the polarization curves, which can be interpreted as local metal depassivation. The absence of a sharp increase in i in this case is apparently due to the repassivation of the arising pits. Passive film breakdown was observed at 0.27 V.

TT of a steel sample without a CIN shifted E_0 and E_{pt} in the negative direction (Table 1). In spite of this, E_{br} shifted anodically. The calculated value of ΔE increased by a factor of 2, which may be explained by a growth of the surface oxide during the TT.

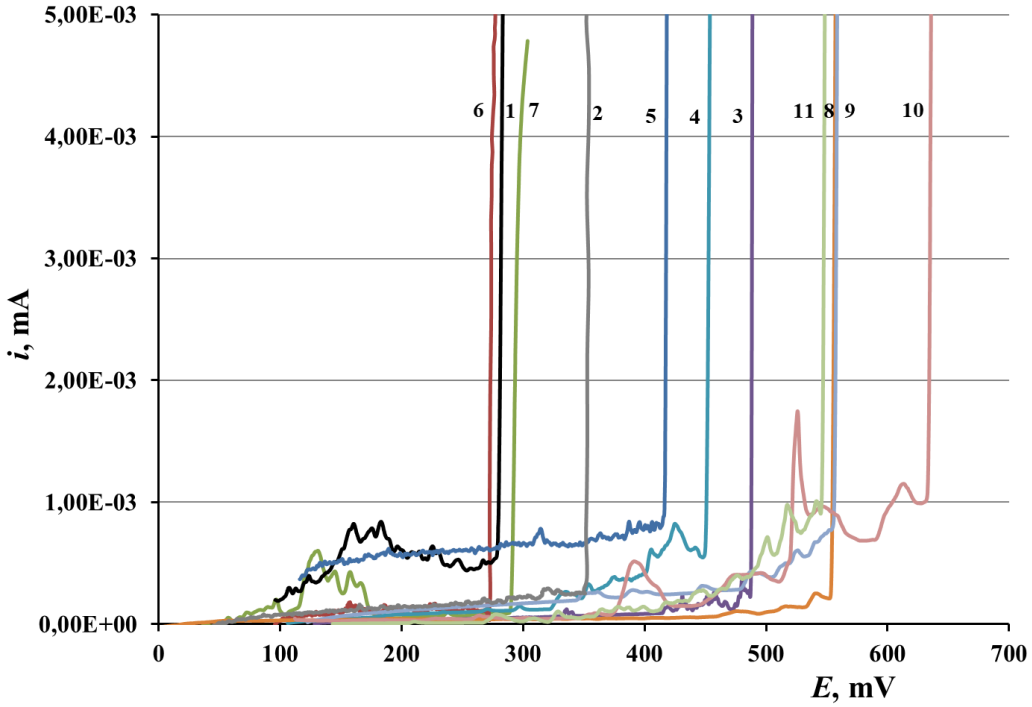

Figure 1. Anodic polarization curves of steel electrode in the IS – 1, after TT without a CIN – 2, after CT in vapors of LA – 3, ODA – 4, BTA – 5, TTA – 6, CBTA – 7, LA+ODA – 8, LA+ ODA+BTA – 9, LA+ODA+TTA – 10, LA+ODA+CBTA – 11.

The steel electrodes treated in LA vapor are characterized by E_0 ennoblement by 0.03 V. The film formed in LA vapor inhibited the anodic dissolution of steel significantly. The metal remained passive up to 0.43 V. Once this E was reached, i oscillations appeared on the polarization curves. The E_{br} of the protective film was around 0.49 V. The ΔE after steel CT by this variant was 0.31 V.

ODA was chosen as the component enhancing the protective effect of LA. The adsorption film obtained in its vapor had almost no effect on the E_0 value. It was close to the value obtained for the sample in the IS. The E_{pt} ranged from 0.3 to 0.35 V. The anti-pitting basis value was nearly the same as the ΔE value for LA. It should be noted that the effect of ODA on the anodic dissolution of steel is similar to that of urotropine [12].

Table 1. Characteristic *E* values of anodic polarization curves of steel after the CT by different variants.

Metal treatment	E_0, V	E_{pt}, V	E_{br}, V	ΔE, V
IS	0.10	0.12	0.27	0.02
TT without CIN	0.05	0.09	0.35	0.04
CT in LA vapors	0.13	0.43	0.49	0.31
CT in ODA vapors	0.11	0.33	0.45	0.32
CT in BTA vapors	0.12	0.13	0.42	0.01
CT in TTA vapors	0.10	0.14	0.27	0.04
CT in CBTA vapors	0.03	0.11	0.29	0.08
CT in LA+ODA mixture vapors	0.02	0.46	0.55	0.44
CT in LA+ODA+BTA mixture vapors	0.12	0.34	0.55	0.22
CT in LA+ODA+TTA mixture vapors	0.11	0.37	0.63	0.26
CT in LA+ODA+CBTA mixture vapors	0.14	0.27	0.63	0.13

The benzotriazoles in question inhibited the anodic process to a smaller extent than LA and ODA. The polarization curves of steel treated in vapors of these compounds were characterized by lower values of E_{pt}, E_{br} and ΔE. BTA itself was an exception, as its E_{br} (0.42 V) was close to those measured for LA and ODA.

The film formed on the surface of a steel electrode in the vapors of the LA+ODA mixture was significantly superior in the protective effect to its components, providing a 1.4 times greater ΔE than the latter. At the same time, the mixture had an effect on the characteristic values of the polarization curves very similar to that of the LA+ODA mixture [12].

Addition of BTA or its derivatives to the LA+ODA binary mixture slightly decreased E_{pt} and the anti-pitting basis. BTA had nearly no effect on E_{br}. TTA and CBTA slightly shifted E_{br} in the anodic direction.

Thus, regardless of the choice of the criterion (E_{pt}, E_{br} or ΔE), the LA+ODA mixture has no striking advantage over the LA+SD mixture but exceeds the protective properties of LA and ODA taken separately. Addition of BTA and its derivatives to the formulation did not cause a significant improvement in the efficiency of the LA+ODA binary CIN.

Additional information about the protective effect of CIN films and its mechanism can be obtained using electrochemical impedance spectroscopy.

2.1.2. Electrochemical impedance spectroscopy

Bode and Nyquist plots of steel electrode in the initial state (IS) are shown in Figure 2. Based on the equivalent circuit used, the hodograph can be divided into 3 sections. The frequency region of 100000 – 1000 Hz characterizes the electrolyte (R_s), that of 1000 – 10 Hz

characterizes the surface film consisting of an airborne oxide (R_{sl}), while the low frequency region (5–0.1 Hz) corresponds to processes related to the double electric layer (R_{ct}).

According to the calculated values (Table 2), the exponential factor for Q_{sl} is 0.75. This indicates the inhomogeneity of the surface oxide layer. The value of n_{dl} is equal to 1, which allows us to interpret the constant phase element of the double layer as pure capacitance. Diffusion processes are missing in this case. The main contribution to the overall corrosion resistance is made by R_{sl} whose value is almost 2 times higher than R_{ct}.

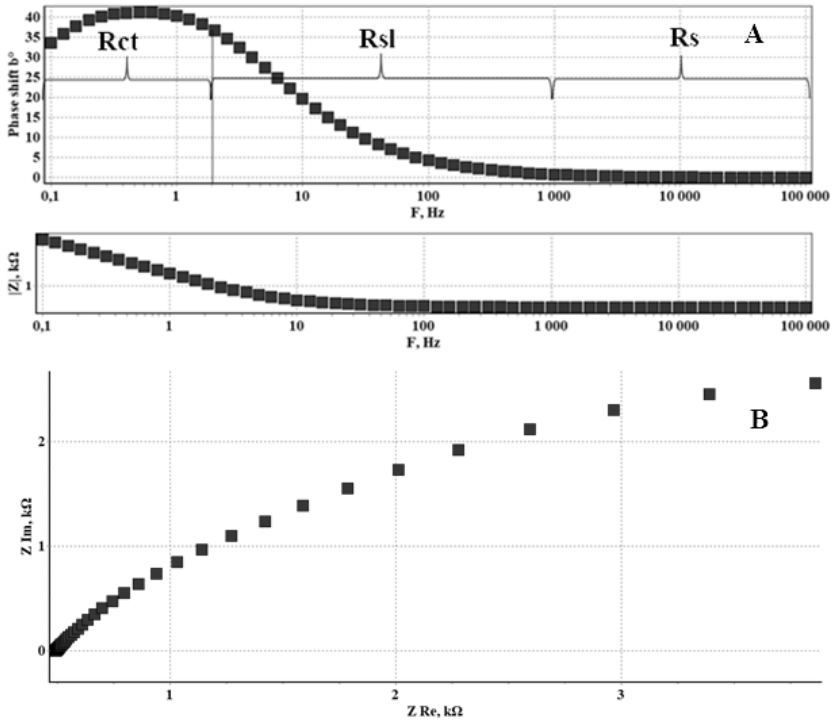

Figure 2. Bode plots (A) and Nyquist plots (B) of a steel electrode in the IS.

The TT of a steel electrode does not change the hodograph shape (Figure 3) but significantly enhances the resistive characteristics of the electrode. The increase in the charge transfer resistance is presumably due to metal oxidation and a decrease in the electrochemically active area of the electrode surface. This is confirmed by a decrease in Q_{dl} values. The heterogeneity of the surface oxide film decreases slightly (n_{sl}=0.87).

The CT in vapors of individual CINs, like the TT without CINs, increased the R_{sl} and R_{ct} values. The shape of the hodograph did not change significantly. The heterogeneity of the surface layer decreased in comparison with the background. The noticeable increase in the complex resistance of the system for samples treated in ODA, TTA, and CBTA vapors occurred due to a significant increase in R_{ct} values compared to R_{sl}. This is probably due to the interaction of these CINs with the surface oxides. After CT of electrodes with LA and BTA, the contributions of R_{ct} and R_{sl} to the complex resistance remained nearly the same.

The values of Q_{sl} and Q_{dl} after CT with all the individual CINs, except for BTA, decreased, which is a consequence of CIN adsorption on the steel surface. In the case of

BTA, the Q_{dl} value after CT remained almost unchanged. In fact, Q_{sl} became the pure capacitance of the surface layers formed in ODA and TTA vapors. In all the cases, except for the films formed in CBTA vapors, Q_{dl} was the pure capacitance of the electrical double layer. A decrease in n_{dl} associated with the inhomogeneity of the oxide-inhibitor layer was observed in the study of CBTA films.

A calculation of Z values indicates that, of the individual compounds studied, ODA (96.6%) and LA (94.8%) are the most efficient compounds in the chamber protection of steel. At the same time, ODA significantly exceeds UR studied previously (84.8%) [12]. BTA and its derivatives did not provide efficient protection.

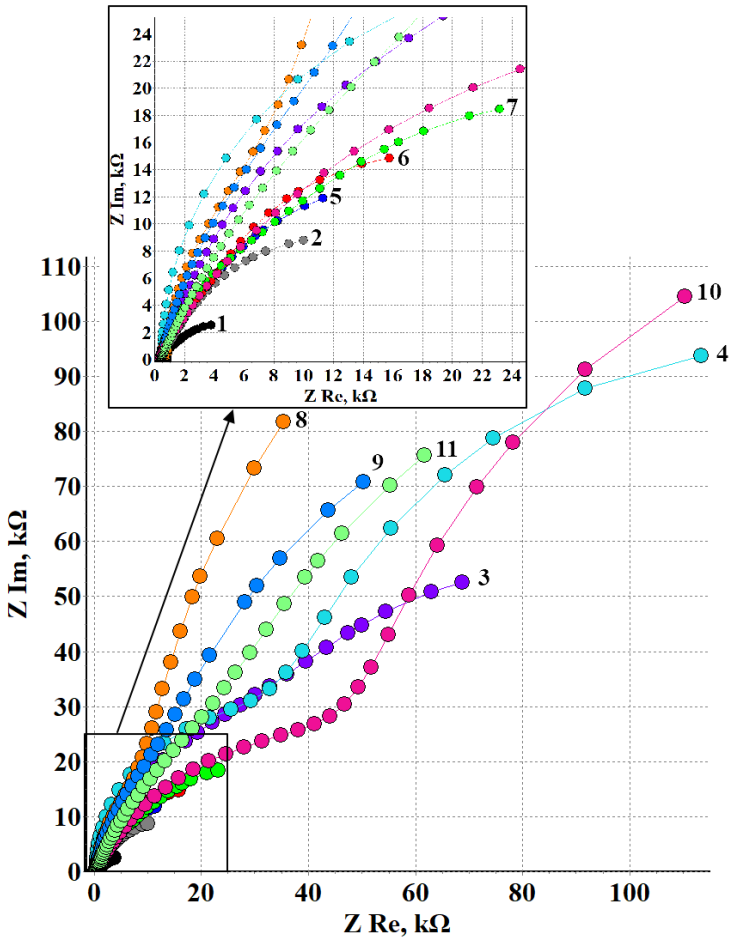

Figure 3. Nyquist plots of steel electrode in IS – 1; after TT without a CIN – 2; CT in the vapors of LA – 3, ODA – 4, BTA – 5, TTA – 6, CBTA – 7, LA+ODA – 8, LA+ODA+BTA – 9, LA+ODA+TTA – 10, LA+ODA+CBTA – 11.

In the hodograph curves corresponding to mixed CIN, the parts responsible for surface layers and polarization resistance became more distinct.

Table 2. Equivalent circuit parameters after various steel electrode treatments.

Metal treatment	R_s kΩ·cm²	Q_{sl}, S·s^n/cm²	n_{sl}	R_{sl} kΩ·cm²	Q_{dl} S·s^n/cm²	n_{dl}	R_{ct} kΩ·cm²	Z,%
IS	0.49	$1.88\cdot10^{-4}$	0.75	5.00	$3.01\cdot10^{-4}$	1	2.61	
TT without a CIN	0.61	$6.75\cdot10^{-5}$	0.87	11.8	$5.46\cdot10^{-5}$	0.95	10.33	65.5
CT in LA vapors	0.57	$6.57\cdot10^{-6}$	0.85	73.13	$2.00\cdot10^{-5}$	1	72.71	94.8
CT in ODA vapors	0.44	$1.94\cdot10^{-6}$	1	54.95	$8.86\cdot10^{-6}$	1	167.1	96,6
CT in BTA vapors	0.39	$5.64\cdot10^{-5}$	0.85	17.54	$5.60\cdot10^{-5}$	1	15.55	76.8
CT in TTA vapors	0.44	$2.52\cdot10^{-5}$	1	8.71	$4.76\cdot10^{-5}$	1	24.22	76.8
CT in CBTA vapors	0.46	$1.90\cdot10^{-5}$	0.9	18.51	$3.96\cdot10^{-5}$	0.86	32.81	85.1
CT in LA+ODA mixture vapors	0.83	$8.58\cdot10^{-6}$	1	35.98	$9.87\cdot10^{-6}$	1	257.23	97,6
CT in LA+ODA+BTA mixture vapors	0.46	$6.81\cdot10^{-6}$	1	34.25	$1.15\cdot10^{-5}$	1	140,3	95,6
CT in LA+ODA+TTA mixture vapors	0.19	$2.32\cdot10^{-6}$	0.7	75.96	$8.55\cdot10^{-6}$	1	256.7	97,7
CT in LA+ODA+CBTA mixture vapors	0.41	$8.65\cdot10^{-6}$	0.77	96.15	$8.4\cdot10^{-6}$	1	188.75	97,3

CT of steel with the LA+ODA mixture resulted in a considerable increase in the hodograph radius, mainly due to the abrupt increase in R_{ct} which was considerably larger than that of individual compounds. It is interesting that in this case, R_{sl} became somewhat smaller than that of the mixture components. The Q_{sl} of the mixed CIN was comparable to the Q_{sl} of ODA films.

The Q_{dl} value for the LA+ODA mixture is significantly smaller than the Q_{dl} for LA but slightly exceeds the Q_{dl} for ODA. At the same time, n_{sl} and n_{dl} are equal to 1, which indicates that the surface film is uniform and the electrode processes in the double layer are not complicated by diffusion.

The Z value for the binary mixture LA+ODA (97.6%) exceeds the Z value of its components and nearly equals the Z value of the LA+UR mixture (96.9%) [12].

The addition of TTA and CBTA to the LA+ODA binary mixture led to an increase in R_{sl} that was more pronounced in the case of CBTA. The R_{ct} values in the ternary mixtures were significantly greater than R_{sl}. At the same time, TTA nearly did not affect the R_{ct} value of the mixed CIN, while BTA and CBTA reduced its value somewhat.

The addition of triazoles to the mixed inhibitor led to a decrease in Q_{sl} in the case of BTA and TTA and had almost no effect on the Q_{sl} value in the case of CBTA. The n_{sl} values in the case of BTA showed a high homogeneity of the surface film formed. The n_{sl} of films formed in ternary mixed CIN containing TTA and CBTA was smaller than 0.8, indicating a heterogeneity of the protective surface films.

The Q_{dl} values of the films formed in ternary mixtures are close to those provided by the LA+ODA binary formulation. The n_{dl} values make it possible to state that the constant phase element of films of these mixed CIN is pure capacitance.

The calculation of Z values indicates that addition of BTA and CBTA to the LA+ODA mixture does not improve the protection efficiency, while TTA improves it insignificantly. Moreover, the ternary mixtures studied here did not have appreciable advantages over the ternary mixtures reported previously [12].

Thus, electrochemical tests failed to reveal any appreciable advantages of formulations containing ODA over similar mixtures containing UR.

In addition, electrochemical impedance spectroscopy allow some initial conclusions about the mechanism of action of the CIN studied to be made. It has been shown previously [3, 7, 12] that one can estimate the contributions of the blocking and activation mechanisms of corrosion inhibition to the protective effect of chemical agents whose EIS spectra can be described by the equivalent circuit used.

It was suggested to estimate the coefficients of corrosion inhibition due to surface blocking (γ_{sl}) by the ratio of R_{sl} resistances of a sample after CT (R_{sl}^{CT}) and in the initial state (R_{sl}^{IS}):

$$\gamma_{sl} = \frac{R_{sl}^{CT}}{R_{sl}^{IS}}$$

Similarly, the coefficients of corrosion inhibition due to changes in the kinetics of electrochemical processes (activation effects, γ_{ct}) can be estimated by the relationship:

$$\gamma_{ct} = \frac{R_{ct}^{CT}}{R_{ct}^{IS}}$$

The γ_{sl} and γ_{ct} values calculated in this way are presented in Table 3. Their analysis shows that all the CIN studied operate by a mixed blocking-activation mechanism of action. However, the activation component clearly predominates. The γ_{ct} values are a few times larger than γ_{sl}.

Thus, the results of impedance measurements correlate well with those of polarization measurements. However, more accurate information about the protective properties of CIN films can be obtained by direct corrosion measurements. In addition, corrosion experiments allow the mutual effect of the components of mixed inhibitors to be estimated quantitatively.

Table 3. Coefficients of steel protection with CIN by the blocking (γ_{sl}) and activation (γ_{ct}) mechanisms.

Metal treatment	γ_{sl}	γ_{ct}
IS	-	-
TT without a CIN	2.4	3.9
CT in LA vapors	14.6	27.9
CT in ODA vapors	11.0	64.0
CT in BTA vapors	3.5	6.0
CT in TTA vapors	1.7	9.3
CT in CBTA vapors	3.7	12.6
CT in LA+ODA mixture vapors	7.2	98.6
CT in LA+ODA+BTA mixture vapors	6.9	53.8
CT in LA+ODA+TTA mixture vapors	15.2	98.4
CT in LA+ODA+CBTA mixture vapors	19.2	72.3

2.2. Corrosion tests

The results of corrosion tests of steel that underwent different variants of surface treatment are presented in Table 4.

On the samples that did not undergo TT, the first corrosion defects appeared as soon as in half an hour of exposure under the test conditions. TT without a CIN had no effect on the corrosion resistance of steel. General corrosion was observed in both cases.

CT in LA vapors increased the time of total protection 144-fold, *i.e.*, to 72 hours. The corrosion defects had the appearance of dark dots. It is noteworthy that their size did not increase for at least 2 weeks of exposure of the samples to the corrosive environment. ODA completely prevented the corrosion of steel under the test conditions for 96 hours. BTA and its derivatives (TTA and CBTA) slightly increased the total protection time compared to the background samples. After 2–4 hours of metal exposure under the test conditions, spots of corrosion products appeared on the metal surface and their area increased with time. In the case of CBTA, dark spots appeared on the surface and their number increased rapidly.

The LA+ODA binary mixture protected steel samples for a considerably longer period (216 hours). Of the ternary formulations, the longest metal protection (696 hours) was provided by the LA+ODA+TTA mixture. The LA+ODA+BTA and LA+ODA+CBTA mixtures showed no advantage over the binary formulation.

Note that the protective properties of the mixed CINs greatly exceeded those of their components. However, their synergistic interaction does not seem to occur. This phenomenon was also observed by us previously [3, 7].

According to [7], estimation of the protective properties of inhibitors based on τ relies on the relationship

$$\tau_{\Sigma,\text{meas.}} > \tau_{\Sigma,\text{calc.}}$$

as a criterion for the synergistic interaction of the mixture components, where $\tau_{\Sigma,\text{meas.}}$ is the time of metal protection by the mixed inhibitor determined experimentally; $\tau_{\Sigma,\text{calc.}}$ is the τ value calculated on the assumption of the lack of mutual effects between the compounds of an *n*-component mixture. $\tau_{\Sigma,\text{calc.}}$ is calculated by the formula:

$$\tau_{\Sigma,\text{calc.}} = \frac{\tau_1\tau_2\ldots\tau_n}{\tau_0^{n-1}},$$

where the $\tau_1, \tau_2, \ldots \tau_n$ values characterize the protective properties of individual compounds that constitute an *n*-component mixture and τ_0 is that of a blank test.

As follows from the data in Table 4, the above inequality is not fulfilled for the mixtures in question. The time of full steel protection by the LA+ODA binary mixture is essentially smaller than $\tau_{\Sigma,\text{ calc.}}=\tau_{LA}\tau_{ODA}/\tau_0$ (13,824 hours). The same is true for all the ternary mixtures.

Thus, the components of the inhibitor mixtures in question not only fail to show a synergistic protective effect but are antagonistic to each other. Such an antagonism may be due to a decrease in the vapor pressure of formulations due to the interaction of bases (ODA) with acids (LA, BTA, TTA, CBTA).

Table 4. Time of full steel protection by individual CINs (τ) and their mixtures ($\tau_{\Sigma,\text{meas.}}$) and $\tau_{\Sigma,\text{calc.}}$ values based on the assumption of no mutual effect of the components of mixed CINs.

Metal treatment	**τ ($\tau_{\Sigma,\text{meas.}}$), *h***	**$\tau_{\Sigma,\text{ calc.}}$, *h***
IS	0.5	–
TT without a CIN	0.5	–
CT in LA vapors	72	–
CT in ODA vapors	96	–
CT in BTA vapors	3	–
CT in TTA vapors	4	–
CT in CBTA vapors	2	–
CT in LA+ODA mixture vapors	216	13824
CT in LA+ODA+BTA mixture vapors	216	82944
CT in LA+ODA+TTA mixture vapors	696	110592
CT in LA+ODA+CBTA mixture vapors	216	55296

However, the protective aftereffect of the CIN mixtures significantly exceeds the aftereffect of their constituents. This confirms once again the conclusion that the synergistic

interaction of components is desirable but not mandatory for the creation of efficient mixed inhibitors [3, 7].

2.3. Ellipsometry

It is noteworthy that the protective effect of the CINs studied is associated with the formation of nanoscale films on a steel surface. This is confirmed by the data given in Table 5.

Upon TT of steel in the absence of a CIN, the thickness of the oxide film on steel increased by 7 nm on average. Addition of the individual inhibitors studied into the chamber noticeably inhibited the oxide growth or terminated it in the case of ODA. At the same time, adsorption films with a thickness from 2.5 nm (TTA) to 11 nm (ODA) formed on the metal.

All the mixed CINs studied prevented oxide growth and formed adsorption films on steel with thicknesses ranging from 10.5 nm (LA+ODA+TTA) to 20 nm (LA+ODA+BTA). No correlation between the protective aftereffect of the films and their thickness was observed in the series of mixed CIN. Nevertheless, all the mixed inhibitors formed adsorption surface layers that were more than 10 nm thick.

Table 5. Thickness of oxide films and CIN adsorption layers after treatment of steel samples in various modes.

Metal treatment	Δ*d* of the oxide film, nm	Δ*d* of the CIN adsorption film, nm
IS	–	–
TT without a CIN	7.0	–
CT in LA vapors	3.5	4.0
CT in ODA vapors	0	11.0
CT in BTA vapors	2.5	5.5
CT in TTA vapors	1.5	2.5
CT in CBTA vapors	3.5	4.0
CT in LA+ODA mixture vapors	0	15.0
CT in LA+ODA+BTA mixture vapors	0	20.0
CT in LA+ODA+TTA mixture vapors	0	10.5
CT in LA+ODA+CBTA mixture vapors	0	11.0

Conclusions

1. The action of lauric acid in the chamber protection of steel can be enhanced by addition of octadecylamine, as well as octadecylamine and benzotriazole or its derivatives such as tolyltriazole or chlorobenzotriazole.
2. All the CINs studied have a blocking-activating mechanism of action, with predominance of the activation component.

3. The protective action of the mixed chamber inhibitors studied is significantly superior to the protective action of their components. Nevertheless, analysis of the mutual effect of the components indicates the lack of their synergistic interactions.
4. Adsorption of the mixed inhibitors studied inhibits or, in the case of octadecylamine and mixed CINs, prevents the oxide growth on steel during CT.
5. During CT of steel by the inhibitors studied, nanosized adsorption films are formed on its surface. There is no unambiguous dependence between their thickness and the protective effect of CIN, but the most efficient inhibitors are characterized by adsorption layers with a thickness of 10 nanometers or more.

References

1. N.N. Andreev, O.A. Goncharova, Yu.I. Kuznetsov and A.Yu. Luchkin, *A method for metal protection from atmospheric corrosion*, RU Patent 2649354, 02.04.2018 (in Russian).
2. O.A. Goncharova, N.N. Andreev, A.Y. Luchkin, Y.I. Kuznetsov, N.P. Andreeva and S.S. Vesely, Protection of copper by treatment with hot vapors of octadecylamine, 1,2,3-benzotriazole, and their mixtures, *Mater. Corros.*, 2018, **70**, 161–168. doi: 10.1002/maco.201810366
3. A.Y. Luchkin, O.A. Goncharova, N.P. Andreeva, V.E. Kasatkin, S.S. Vesely, Y.I. Kuznetsov and N.N. Andreev, Mutual Effects of Components of Protective Films Applied on Steel in Octadecylamine and 1,2,3-Benzotriazole Vapors, *Materials*, 2021, **14**, 7181. doi: 10.3390/ma14237181
4. Hong-Liang Zhang, Teng-Fei Ma, Li-Xin Gao, Da-Quan Zhang, Guo-An Wei, Hong-Bin Yan and Shi-Li,Vapor phase assembly of urea-amine compounds and their protection against the atmospheric corrosion of carbon steel, *J. Coat. Technol. Res*., 2020, **17**, 503–515. doi: 10.1007/s11998-019-00301-7
5. Hong-Liang Zhang, Da-Quan Zhang, Li-Xin Gao, Yan-Yan Liu, Hong-Bin Yan, Shi-Li Wei and Teng-Fei Ma, Vapor phase assembly of benzotriazole and octadecylamine complex films on aluminum alloy surface, *J. Coat. Technol. Res*., 2021,**18**, 435–446. doi: 10.1007/s11998-020-00405-5
6. O.A. Goncharova, Yu.I. Kuznetsov, N.N. Andreev, A.Yu. Luchkin, N.P. Andreeva and D.S. Kuznetsov, A new corrosion inhibitor for zinc chamber treatment, *Int. J. Corros. Scale Inhib*., 2018, **3**, 340–351. doi: 10.17675/2305-6894-2018-7-3-5
7. O.A. Goncharova, A.Y. Luchkin, N.P. Andreeva, V.E. Kasatkin, S.S. Vesely, Y.I. Kuznetsov and N.N. Andreev, Mutual Effect of Components of Protective Films Applied on Copper and Brass from Octadecylamine and 1,2,3-Benzotriazole Vapors, *Materials*, 2022, **15**, 1541. doi: 10.3390/ma15041541
8. A.Y. Luchkin, O.A. Goncharova, I.A. Arkhipushkin, N.N. Andreev and Yu.I. Kuznetsov, The effect of oxide and adsorption layers formed in 5-Chlorobenzotriazole vapors on the corrosion resistance of copper, *J. Taiwan Inst. Chem. Eng*., 2020, **117**, 231–241. doi: 10.1016/j.jtice.2020.12.005

9. O.A. Goncharova, A.Yu. Luchkin, Yu.I. Kuznetsov, N.N. Andreev, N.P. Andreeva and S.S. Vesely, Octadecylamine, 1,2,3-benzotriazole and a mixture thereof as chamber inhibitors of steel corrosion, *Int. J. Corros. Scale Inhib*, 2018, **2**, 203–212. doi: 10.17675/2305-6894-2018-7-2-7
10. A.Yu. Luchkin, O.A. Goncharova, N.N. Andreev, I.A. Arkhipushkin, L.P. Kazanskiia and Yu.I. Kuznetsov, 5-Chloro-1,2,3-benzotriazole as a Chamber Corrosion Inhibitor for the MA8 Magnesium Alloy, *Prot. Met. Phys. Chem. Surf*., 2021, **57**, 1319–1327. doi: 10.1134/S2070205121070108
11. O.A. Goncharova, A.Yu. Luchkin, I.N. Senchikhin, Yu.B. Makarychev, V.A. Luchkina, O.V. Dement'eva, S.S. Vesely and N.N. Andreev, Structuring of Surface Films Formed on Magnesium in Hot Chlorobenzotriazole Vapors, *Materials*, 2022, **15**, 6625. doi: 10.3390/ma15196625
12. I.V. Tsvetkova, A.Yu. Luchkin, O.A. Goncharova, S.S. Veselyi and N.N. Andreev, Chamber inhibitors of steel corrosion based on lauric acid, *Int. J. Corros. Scale Inhib*., 2021, **10**, 107–119. doi: 10.17675/2305-6894-2021-10-1-6
13. GOST 380-2005, *Common Quality Carbon Steel*. *Grades* (in Russian).
14. E. Kondoh, *ELLIPSHEET: Spreadsheet Ellipsometry (Excel Ellipsometer)*. https://www.ccn.yamanashi.ac.jp/~kondoh/ellips_e.html.

♦ ♦ ♦